Advances in Science and Technology Research Journal

Advances in Science and Technology Research Journal 2024, 18(2), 284–295
https://doi.org/10.12913/22998624/184341
ISSN 2299-8624, License CC-BY 4.0

Received: 2023.12.11
Accepted: 2024.02.20
Published: 2024.03.14

Effect of Regular Shot Peening and Semi-Random Shot Peening Conditions on Selected Properties of the Surface Layer of Gray Cast Iron

Agnieszka Skoczylas[1*], Kazimierz Zaleski[1]

[1] Department of Production Engineering, Mechanical Engineering Faculty, University of Technology, ul. Nadystrzycka 36, 20-618 Lublin, Poland

* Corresponding author's e-mail: a.skoczylas@pollub.pl

ABSTRACT

Both dispersed and concentrated shot peening can be an effective method for the finishing of machine components. This work investigates the effect of two different shot peening (SP) processes conducted with the same technological parameters on selected properties of the surface layer of gray cast iron EN-GJL 250. Specifically, regular shot peening (RSP) and semi-random shot peening (SRSP) were investigated in the study. The results demonstrated that the surface quality of EN-GJL 250 samples was higher after RSP than after SRSP. The analyzed surface roughness parameters were lower after RSP than after SRSP, with the exception of the *Rvk* parameter. As a result of RSP, the analyzed roughness parameters increased from 5% to 62% in relation to their values after pre-treatment. The lowest values of the surface roughness parameters were obtained after RSP conduced with the impact energy E = 100 mJ, the distance between the dimples x = 0.3 mm, and the diameter of the shot peening element d = 14.3 mm. Assessment of the 3D surface topography showed significant differences in the formation of machining traces depending on the employed surface treatment. In RSP, the traces were arranged in a uniform manner, with the assumed step, whereas in SRSP the shot peening traces had no set pattern of orientation. The application of RSP and SRSP caused an increase in surface microhardness. The maximum surface microhardness was 75 HV0.5 for RSP and 98 HV0.5 for SRSP. Residual stresses were higher after SRSP than after RSP. Compressive residual stresses were induced in both types of shot peening process.

Keywords: regular shot peening, semi-random shot peening, gray cast iron, surface roughness, microhardness, residual stress.

INTRODUCTION

Shot peening (SP) and burnishing (B) are finishing methods for machine components, and they are primarily employed to improve operational properties of these components. The use of shot peening and burnishing makes it possible to increase fatigue strength [1, 2]. Their use also makes it possible to increase tribological wear resistance [3] and corrosion resistance [4]. Burnishing and shot peening differ in the way the burnishing element affects the workpiece surface. In burnishing, the tool (e.g. a rotating roller or sliding spherical bowl) is pressed against the workpiece with an approximately constant force [5–7]. The effects of burnishing and shot peening can be assessed by both experimental testing and numerical modeling [8÷10]. Burnishing can also be combined with machining [11]. In shot peening, the peening element hits the workpiece surface [12]. Due to the impact of the shot peening element, traces are formed on the surface of this object. Shot peening kinematics is characterized by regular impacts of the peening element, which results in the formation of successive traces with a constant pitch. This type of shot peening is called concentrated shot peening. An example of concentrated shot peening can be impulse shot peening [13] or centrifugal shot peening [14]. Shot peening can also be a result of impacts exerted on the machined surface by free peening elements (usually balls or shot).

This type of shot peening process is performed on jet [15] or vibratory devices [16, 17] and is known as dispersed shot peening. Brushing has features of both concentrated and dispersed shot peening [18, 19].

In dispersed shot peening, the peening elements hit the surface randomly, causing the formation of dimples on the machined surface that are located at different distances from each other. An increase in the shot peening time leads to an increase in the coverage of the shot peened surface with the dimples. In both jet and vibratory shot peening processes, the shot peening elements move in different directions at different speeds. In order to enable dispersed shot peening with a known impact energy and a known topography of dimple distribution, a method of semi-random shot peening (SRSP) was developed [20, 21].

Burnishing and shot peening are usually employed for machining elements made of materials with high ductility, such as steel [22], aluminum alloys [23], and titanium alloys [24]. However, a vast number of elements exposed to variable operational loads and tribological wear are made of cast iron. Examples of such elements include shafts, cylinders, bodies, slideways, and gears. Therefore, research on the effectiveness of shot peening for cast iron objects was undertaken. A study [25] has shown that shot peening conducted with an intensity of 0.30 mmA causes an increase in the fatigue strength of ductile iron castings, for the as-cast surface and the machined surface a like. A beneficial effect of SP on the fatigue strength and the reduction of casting defects on the surface has been reported in [26]. However, with considerable casting defects, the shot peening induced fatigue strength increase in cast iron elements is negligible [27]. A work by Bagherifard et al. has shown that severe SP of nodular cast iron samples results in a greater increase in their fatigue strength than that observed after conventional shot peening [28]. An increase in fatigue life as a result of SP has also been reported for austempered ductile iron [29]. According to Silva et al. [30] the shot peening of ductile cast iron causes surface layer hardening and leads to increased surface roughness, which is undesired due to the resulting durability of the tested material. It has been shown that the removal of a material layer with a thickness of about 20 μm leads to reduced surface roughness, which results in an increase in wear resistance [30]. The impact of shot peening on wear resistance has also been studied in [31, 32]. A beneficial influence of SP on the surface layer properties of laser-quenched cast iron has been demonstrated in [33]. Maleki used artificial neural network modeling to investigate the severe shot peening of nodular cast iron with the ferrite-pearlite matrix [34]. Feng et al. have shown that laser shock peening also has a beneficial effect on the surface layer properties and abrasion resistance of high-chromium cast iron [35].

A study [21] has shown that the use of semi-random shot peening (SRSP) makes it possible to compare the surface layer properties of aluminum alloy obtained after dispersed and concentrated shot peening processes conducted with the same technological parameters. A review of the literature has shown that favorable changes in the surface layer condition can also be obtained by shot peening low-ductility materials such as cast iron. The purpose of this study is to assess changes in properties of the surface layer of gray cast iron samples that were shot peened by the dispersed and concentrated methods, using the same values of impact energy, shot peening element diameter and impact density.

RESEARCH METHODOLOGY

Samples made of gray cast iron EN-GJL 250 (Table 1) were used in the study. EN-GJL 250 is characterized by good casting properties and good machinability. Its production cost is relatively low. Disadvantages of the EN-GJL 250 gray cast iron include low strength, low ductility and poor abrasion resistance. Advantages of this material include excellent noise and vibration damping properties. This material is used in the railway, machine (body casting) and automotive industries. Prior to shot peening, the EN-GJL 250 gray cast iron samples were ground. Peripheral grinding was performed on the SPC-20 grinder with the A-46-KVBE-33 grinding wheel with dimensions of 200×20×51 mm, using the following technological parameters: a grinding depth of a_p = 0.3 mm, a feed speed of v_f = 15 mm/min, and a rotational speed of the grinding wheel of n = 3000 rev/min.

Shot peening was performed on a specially designed test stand. In the experiment, two methods of applying dimples were used. The first one was semi-random shot peening (SRSP), which was implemented in such a way that the dimples

Table 1. Chemical composition and selected properties of gray cast iron EN-GJL 250, according to PN-EN 1561: 2012

Element	C	Si	Mn	S	P	Fe
Content [% weight]	3.00÷3.25	1.85÷2.10	0.40÷0.75	max 0.12	max 0.25	the rest
Tensile strength R_m, MPa				250÷350		
Offset yield point $R_{p0.1}$, MPa				165÷228		
Hardness *HB* 30				145÷215		
Elongation *A*, %				0,3÷0,8		
Young's modulus *E*, GPa				103÷118		
Fracture toughness K_{IC}, MPa				480		

were created at much greater distances than their diameter in the initial phase of the process and became compacted with the peening time. The other method of covering the surface with dimples involved applying dimples one next another with the assumed step *x*. This was a standard shot peening technique known as regular shot peening (RSP). Both methods of forming dimples have been described in detail and shown schematically in [21].

The experiment was conducted according to the research plan specified in Table 2. The variable parameters of the SRSP and RSP processes were: the impact energy (*E*), the diameter of the shot peening element (*d*) and the distance between the impact traces (*x*). Impact energy could be made variable thanks to the use of a cam mechanism and springs in the device. The exchangeable head allowed the use of a peening element of different diameters. The CNC table performed feed motion according to the assumed program at a fixed speed. The speed of the feed motion affected the value of shot peening density *j* (the number of impacts per unit area – Eq. 1).

$$j = \frac{1}{x^2}\ [mm^{-2}] \tag{1}$$

Hommel-Etamic's T800 RC120-400 was used to measure roughness and surface topography. The measurements were made in accordance with EN ISO 25178-2:2022 and EN ISO 21920-2:2022. A TKU300 measuring tip equipped with a measuring needle with a radius r_k = 5 μm was used. The sampling length was *lr* = 0.8 mm, while measuring length *ln* = 4.8 mm. The surface roughness measurement speed was v_t = 0.50 mm/s.

The analyzed surface roughness parameters are widely used in engineering practice, while the parameters related to the Abbott-Firestone curve allow for the assessment of functional characteristics of the surface. The scanned surface area was 1.5×1.5 mm. Surface microhardness was measured by the Vickers method using the Leco LM 700 at microhardness tester. The indenter weight was 500 g (HV 0.5). Residual stresses were measured by X-ray diffraction using a portable diffractometer, Theta-Theta EDGE. Measurements were made in one direction. A chrome lamp was used as the XRD beam source and a vanadium filter was utilized. A 0.5 mm collimator was used. The material model from the system library was used for measurements, it was "Class30_GreyCastIron". The inter-measurement angle was 9°. The XRD beam exposure time was 60 s.

Figure 1 presents an overview of the research methodology and test stands that were used to perform semi-random shot peening and regular shot peening.

Table 2. Technological parameters of SRSP and RSP

No.	*E*, mJ	*d*, mm	*x*, mm	*j*, mm^{-2}
1	15	10	0.30	11
2	100			
3	185			
4	100	3.95		
5		14.3		
6		10	0.15	44
7			0.60	3

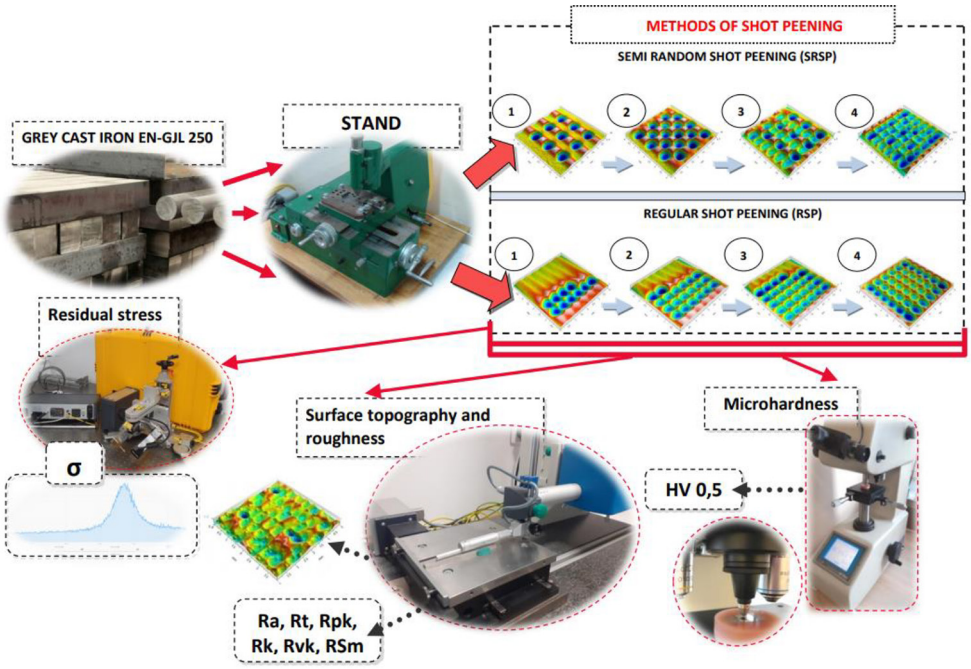

Fig. 1. Methodology of semi-random shot peening and regular shot peening for gray cast iron EN-GJL 250

RESULTS AND DISCUSSION

Measurement surface roughness and topography

Figure 2 shows the influence of energy on the parameters *Ra* and *Rt*. For the surfaces subjected to RSP, there are no clear differences in the values of *Ra* and *Rt* as a function of the applied energy. Regarding SRSP, the use of a higher energy value results in an increase in the tested surface roughness parameters. This increase can be explained by the fact that the higher impact energy leads to more intense deformation, which – in turn – results in a higher strain of the EN-GJL 250 cast iron surface after grinding. The use of RSP leads to an increase in both *Ra* (from 7% to 12%) and *Rt* (from 5% to 14%) with respect to their values after grinding. The changes in the parameters *Ra* and *Rt* as a function of the impact energy after the SRSP process and their absence after RSP can be explained by the differences in dimple application in these processes, which, combined with the impact energy used in the SRSP experiment, can induce significant changes in surface quality.

An increase in the diameter of the ball *d* used in the experiment leads to a decrease in the curvature of the peening element, which results in the

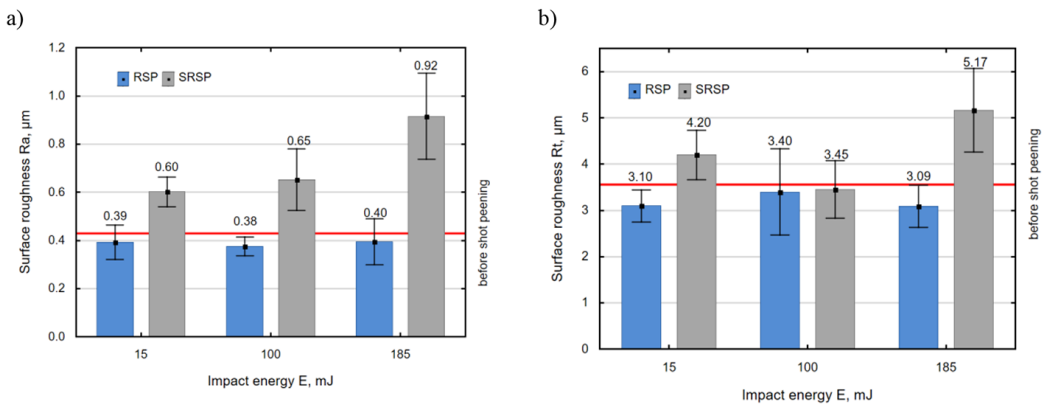

Fig. 2. Influence of the impact energy *E* on the surface roughness parameters *Ra* (a) and *Rt* (b) after RSP and SRSP (d = 10 mm, x = 0.3 mm)

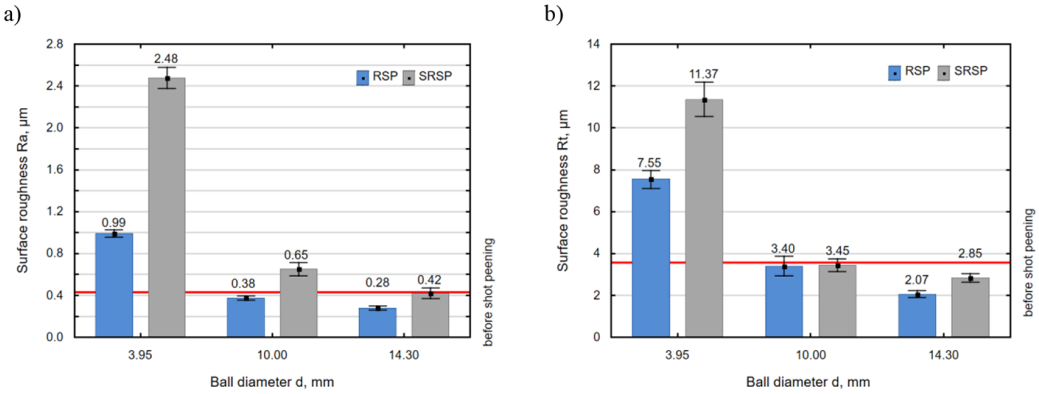

Fig. 3. The surface roughness parameters *Ra* (a) and *Rt* (b) after RSP and SRSP in the function of the ball diameter *d* (*E* = 100 mJ, *x* = 0.3 mm)

formation of dimples with smaller depths on the surface. The formation of less deep traces on the surface only causes levelling and smoothing of micro-irregularities after grinding, which results in a decrease parameters (Fig. 3). The use of the balls with diameters *d* = 10 mm and *d* = 14.3 mm causes a reduction in the *Ra* parameter after RSP and SRSP a like. For both shot peening methods, the use of the ball with a diameter of *d* = 3.95 mm causes the tested roughness parameters to increase due to a smaller contact area between the ball and the sample surface, which leads to more intense plastic-elastic deformation.

Figure 4 presents the effect of the distance between the dimples on the surface roughness parameters *Ra* and *Rt*. As expected, the use of a larger distance between the dimples results in a reduced degree of coverage and thus in more uneven deformation of the machined surface, and, consequently, in reduced surface quality. The best results (the lowest values of *Ra* and *Rt*) were obtained in the regular shot peening process conducted with *x* = 0.3 mm. Figure 5 presents the effect of the technological parameters of RSP and SRSP on the surface roughness parameter *RSm*. As expected, after both processes the micro-irregularities are spaced at a greater distance than after grinding. For all analyzed cases, the *RSm* parameter is higher after SRSP than after RSP, sometimes even more than twice. In SRSP, the surface of the workpiece material is deformed unevenly with multiple shots over a short period of time, which promotes the material flow and the formation of micro-irregularities with a greater spacing. In RSP, the surface is deformed in a controlled way (dimples are applied one next to another), which limits the "movement" of the material. The profiles shown in Table 3 confirm the above-observed changes.

A comparison of these results with the results of previous studies [13, 21] devoted to the RSP and SRSP methods reveals that the *Ra* parameter of the EN-GJL 250 cast iron samples after RSP is lower than that obtained for the shot-peened

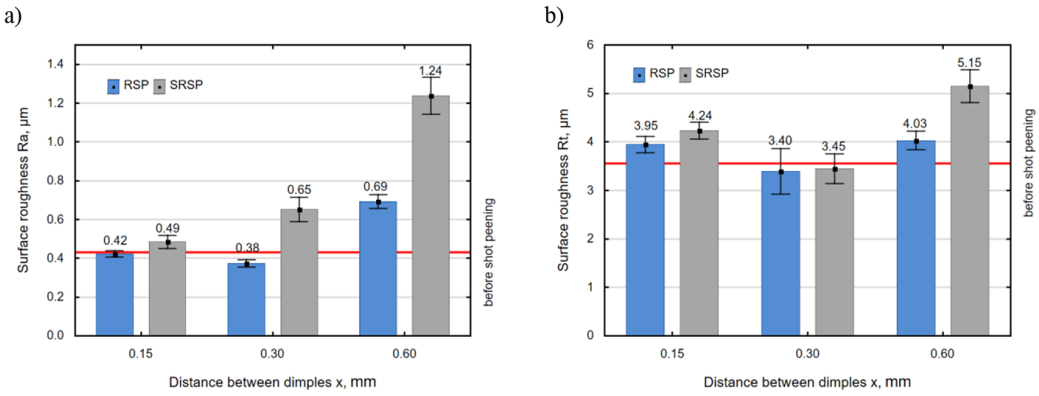

Fig. 4. The surface roughness parameters *Ra* (a) and *Rt* (b) after RSP and SRSP in the function of distance between dimples *x* (*E* = 100 mJ, *d* = 10 mm)

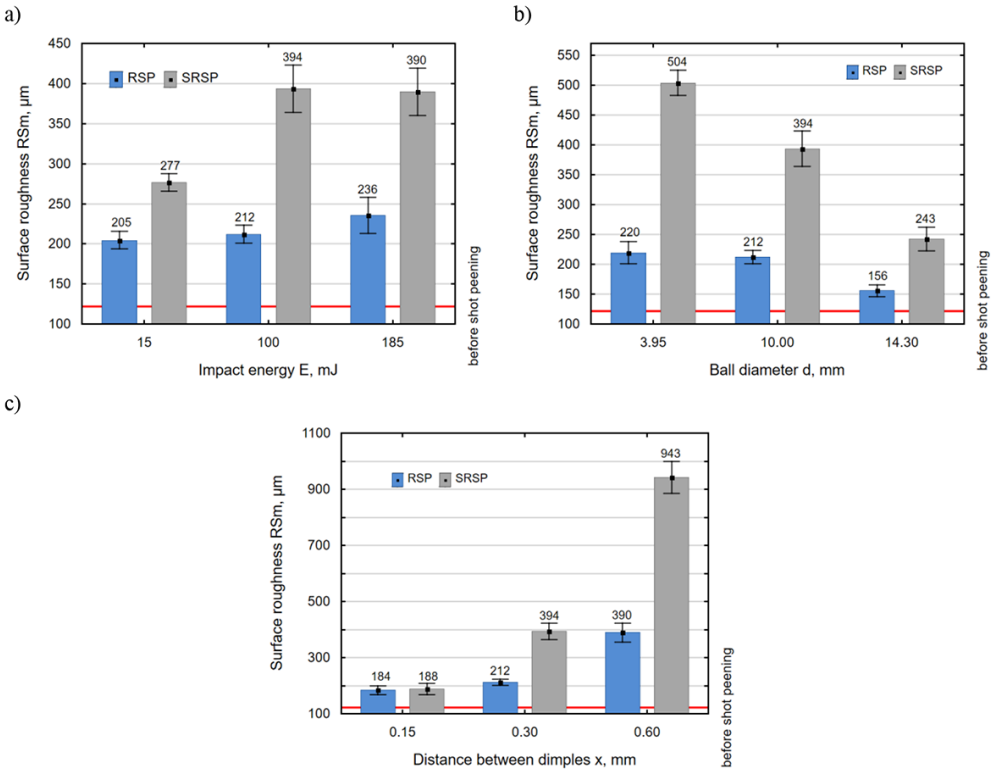

Fig. 5. Influence of the energy *E* (a), ball diameter *d* (b) and distance between dimples *x* (c) on the surface roughness parameter *RSm*

Table 3. Surface profiles after RSP (a) and SRSP (b) (*E* = 100 mJ, *d* = 10 mm, *x* = 0.60 mm)

a)	b)
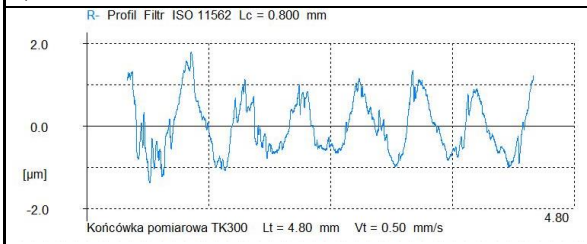	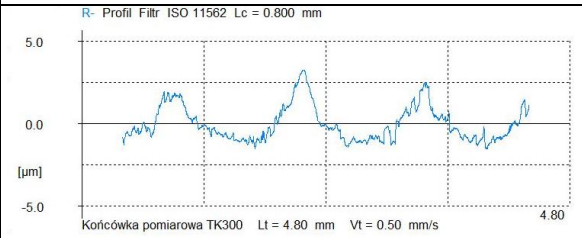
Ra = 0.57 µm; *Rt* = 3.17 µm; *RSm* = 383 µm	*Ra* = 0.87 µm; *Rt* = 4.81 µm; *RSm* = 884 µm

EN-AW 7075 aluminum alloy [21], while for some conditions the *Ra* values are similar to those obtained after impulse shot peening of the Inconel 718 alloy [13]. The effect of the tested technological parameters (*E*, *d*, *x*) on the surface roughness of EN-GJL 250 is similar to that described in [13] and [21]. Referring the present results to those obtained in other studies on shot peening of cast iron, one can observe that the *Ra* and *Rt* parameters decrease for some technological parameters of RSP and SRSP, while in studies [30] and [36] the use of SP led to rise in surface roughness.

In terms of mating between two elements, the important surface roughness parameters allowing the evaluation of these characteristics are the Abbott-Firestone parameters, which are presented in Figures 6÷8 as a function of the applied technological parameters of shot peening. Regardless of the shot peening conditions used, the parameters *Rpk* (reduced peak height) and *Rk* (core depth) are lower after RSP than after SRSP, the exception being the parameter *Rvk* (reduced valley depth). This means that deeper dimples are formed on the shot-peened surface after RSP than after SRSP, and thus they may be potential lubrication pockets. The higher *Rvk* values after RSP result from the method in which dimples are applied: one next to another, with the

assumed step. This way of covering the surface with dimples causes the material to be multiply deformed over a small area and within a short period of time, making it "spring back", which results in a greater share of plastic-elastic strains. Compared to its value after grinding, the *Rpk* parameter, which indicates any increase in the wear resistance of the machined surface, is decreased after RSP conducted with the following parameters: $E = 15 \div 185$ mJ, d = const. = 10 mm, x = const. = 0.3 mm. On the other hand, compared to its value after grinding, the *Rpk* parameter shows a 15% decrease after the SRSP process conducted with $E = 100$ mJ, $d = 14.3$ mm and $x = 0.3$ mm. It can be observed that the surface load capacity, which is defined by the *Rk* parameter and shows whether a significant area of the surface is in contact with the surface of the mating element after a running-in period, improved after the RSP process conducted with the impact energy ranging $E = 15 \div 185$ mJ ($d = 10$ mm, $x = 0.3$ mm) and the ball with $d = 14.3$ mm ($E = 100$ mJ, $x = 0.3$ mm). The use of the ball with $d = 3.95$ mm ($E = 100$ mJ, $x = 0.3$ mm) in the RSP and SRSP processes causes larger depressions to be "knocked out" on the machined surface, which results in reduced surface quality. Nonethless, there is an improvement in the retention capacity of the lubricant.

The experimental results demonstrate that the functional parameters *Rpk* and *Rk* for the selected shot peening conditions increased from 15% to 62% in relation to their values after grinding. These changes are smaller than those reported in [2] and [14], which may result from the fact that the workpiece and pre-treatment types used in this study differed from those employed in [2,

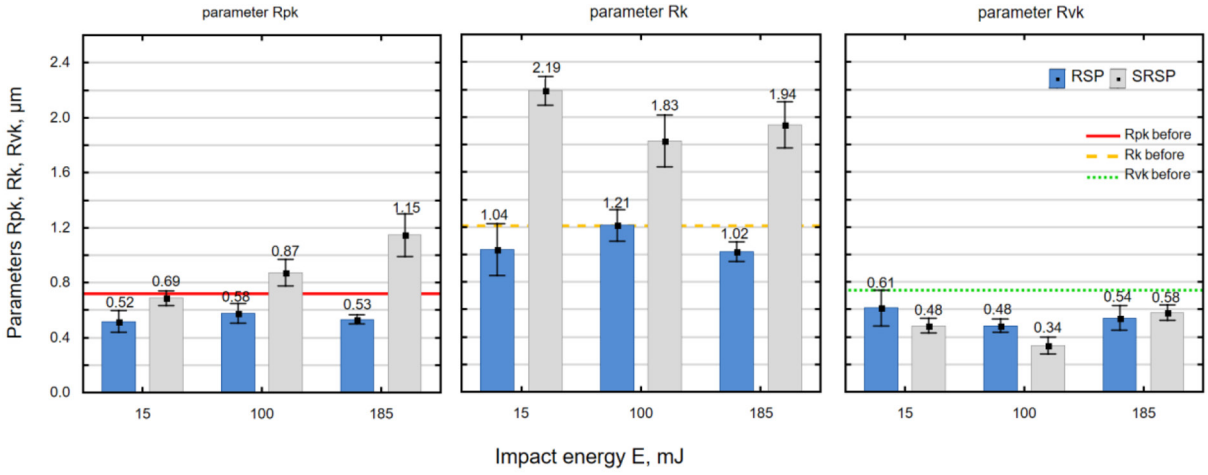

Fig. 6. Effect of the impact energy E on the Abbott-Firestone curve parameters after RSP and SRSP ($d = 10$ mm, $x = 0.3$ mm)

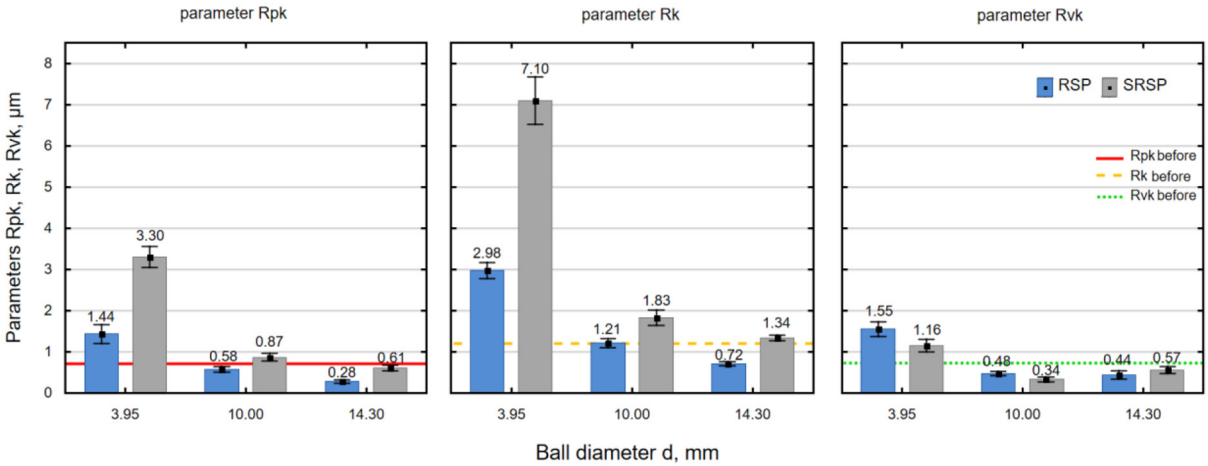

Fig. 7. Effect of the ball diameter on the Abbott-Firestone curve parameters after RSP and SRSP ($E = 100$ mJ, $x = 0.3$ mm)

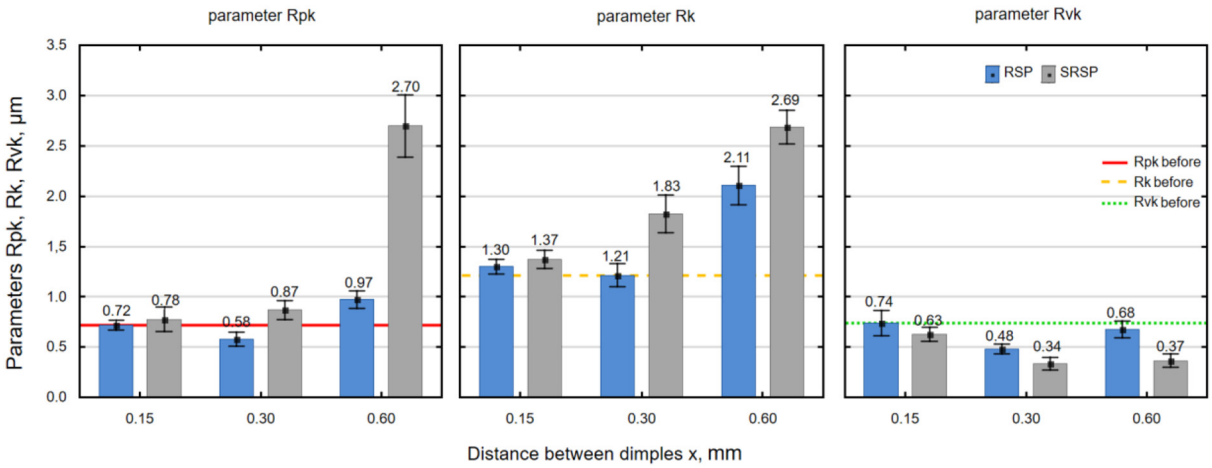

Fig. 8. Effect of the distance between dimples x on the Abbott-Firestone curve parameters after RSP and SRSP (E = 100 mJ, d = 10 mm)

14]. The surface roughness results are confirmed by the obtained surface topography (Table 4). On the surface subjected to RSP, the traces are arranged evenly, at regular intervals, with the assumed step. Regarding the surface after SRSP, the dimples do not have a set pattern. The method of surface treatment affects the deformation of surface micro-irregularities after grinding. The 3D parameters are lower after RSP than after SRSP, which is the same trend as that observed for the 2D surface roughness parameters.

Microhardness

The cyclic impact of the ball on the surface of the sample leads to an increase in the density of dislocations. The movement of the dislocations is stopped when they come across grain boundaries and precipitations, which results in an increase in surface microhardness. Both RSP and SRSP cause the surface microhardness to increase. The maximum surface microhardness increase is 75 HV0.5 for RSP and 98 HV0.5 for SRSP. These maximum microhardness values are greater than those obtained after RSP and SRSP for the elements made of aluminum alloy EN-AW 7075 [21].

The effect of the technological parameters of shot peening on the microhardness of gray cast iron EN-GJL 250 after the RSP and SRSP processes is plotted in Figures 9 ÷ 11. For the impact energy range E = 15 ÷ 100 mJ, there are no clear changes in surface microhardness, which suggests that the applied impact energy is too low to cause deformation and dislocation mobility. However, the use of a higher impact

Table 4. Surface topography and 3D surface roughness parameters after regular shot peening (a) and semi-random shot peening (b) (E = 100 mJ, d = 10 mm, x = 0.3 mm)

a)	b)
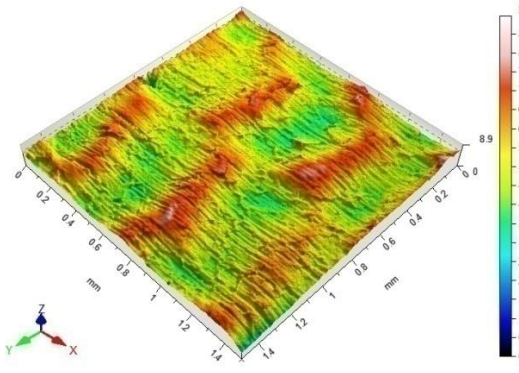	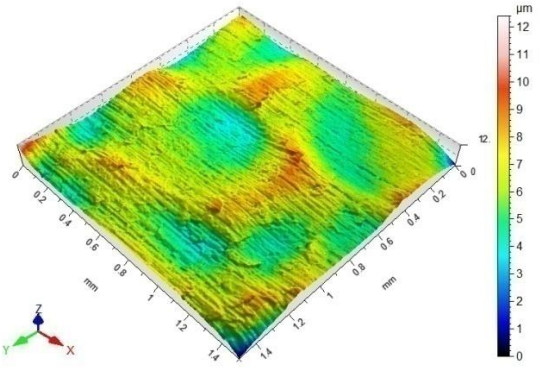
Sa = 0.73 µm; *Sz* = 8.97 µm; *Sp* = 3.71µm; *Sv* = 5.26 µm; *Ssk* = 0.286; *Sku* = 2.75	*Sa* = 0.88 µm; *Sz* = 12.4 µm; *Sp* = 6.31 µm; *Sv* = 6.09 µm; *Ssk* = 0.069; *Sku* = 2.89

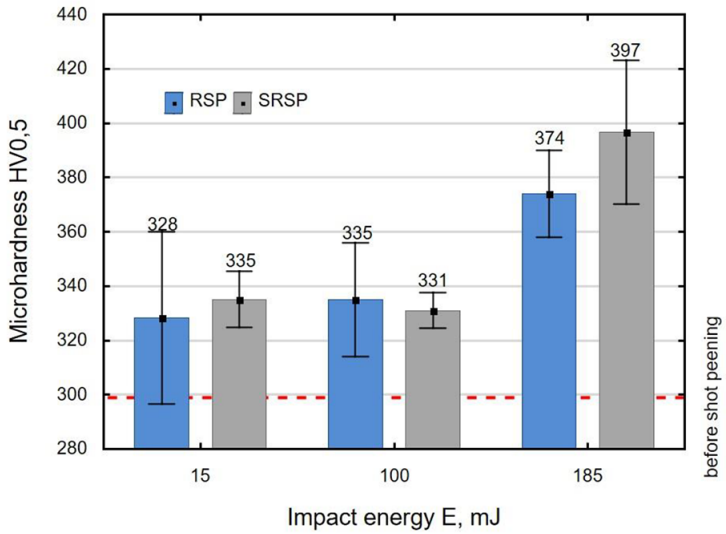

Fig. 9. Effect of the impact energy E on the microhardness of EN-GJL 250 gray cast iron after RSP and SRSP (d = 10 mm, x = 0.3 mm)

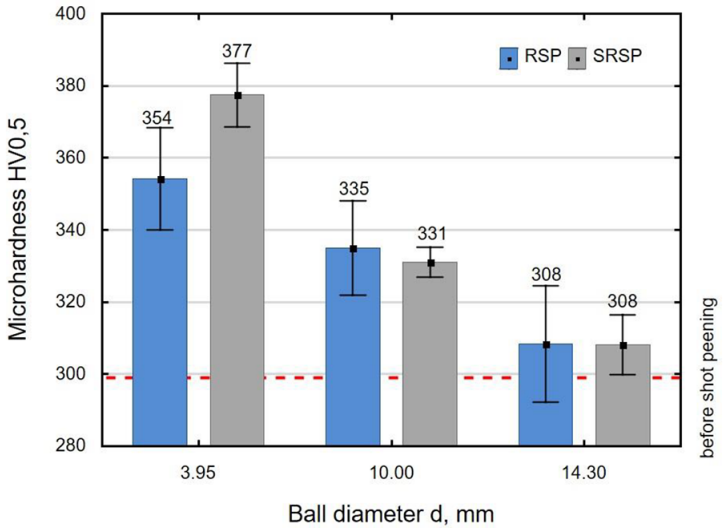

Fig. 10. Effect of the ball diameter d on the microhardness of gray cast iron EN-GJL 250 after RSP and SRSP (E = 100 mJ, x = 0.3 mm)

energy of E = 185 mJ causes marked changes in the surface microhardness (Fig. 9). An increase in the ball diameter used in the experiment causes an increase in the indentation field resulting from the impact, as confirmed in [21]. In effect, the concentration of energy transferred to the sample decreases, which results in reduced microhardness (Fig. 10).

An increase in the distance between the shot impact traces results in a reduced coverage of the machined surface. The uneven deformation of the surface results in reduced microhardness (Fig. 11). A four-fold increase in the distance between the dimples causes the microhardness to decrease by 46 HV0.5 for the RSP method and by 69 HV0.5 for the SRSP method. The microhardness results demonstrate that the greatest changes in their values compared to those observed after grinding occur for the extreme shot peening conditions (E = 185 mJ, d = 3.95 mm, x = 0.15 mm).

Measurement residual stress

Figure 12 shows the effect of the technological parameters of RSP and SRSP on the residual stress on the surface of EN-GJL 250. Compressive stresses occur regardless of the

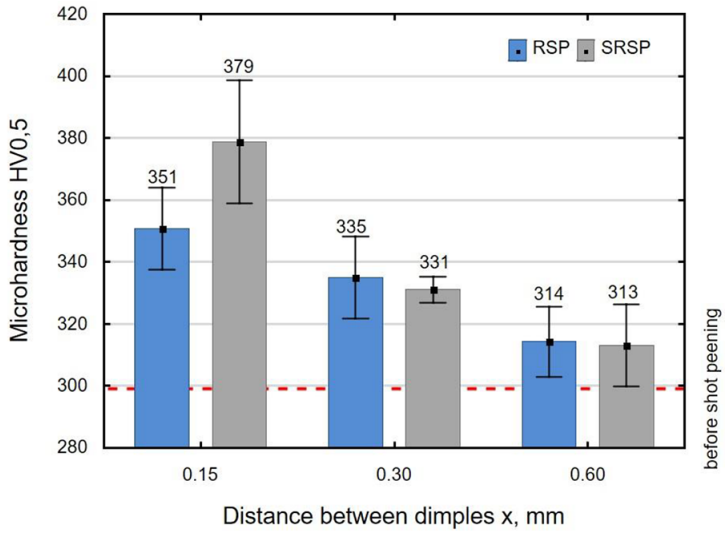

Fig. 11. Microhardness of the surface of gray cast iron EN-GJL 250 after RSP and SRSP carried out with variables distance between dimples x (E = 100 mJ, d = 10 mm)

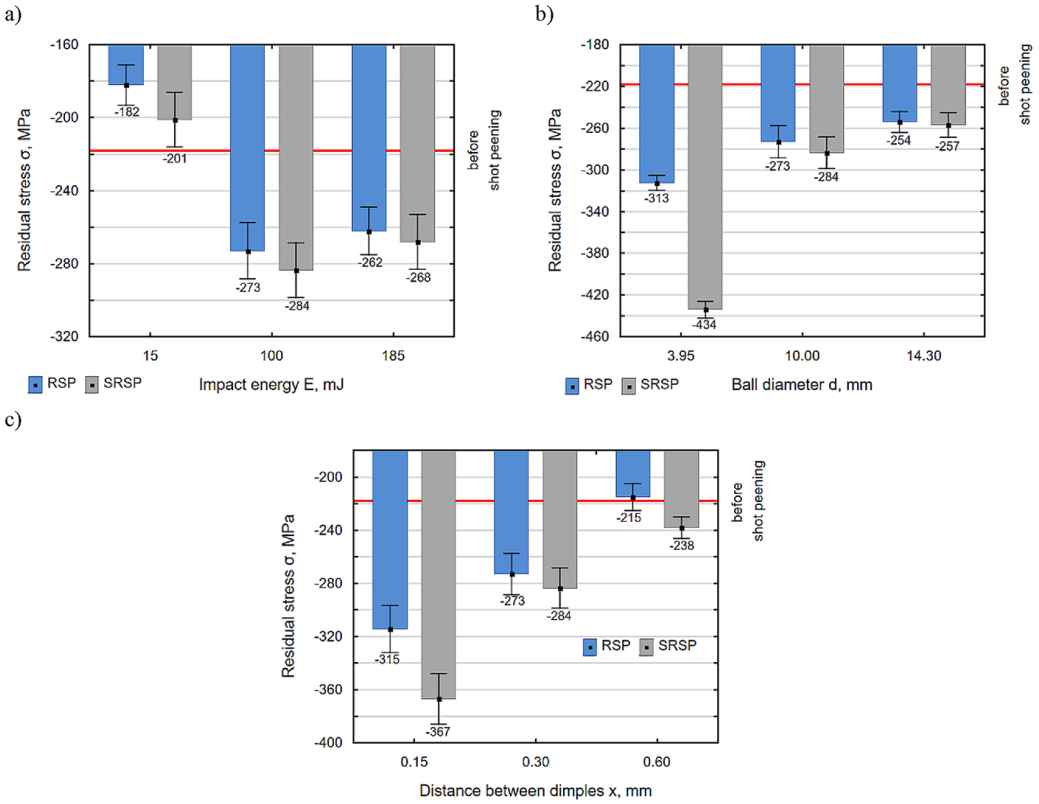

Fig. 12. Effect of the impact energy E (a), ball diameter d (b) and distance between dimples x (c) on the residual stress σ

shot peening method used. As expected, higher stress values are obtained after SRSP than after RSP. The maximum residual stress after SRSP is 16% higher than the maximum stress value after RSP. The largest differences in the residual stress values can be observed for the extreme shot peening conditions (E = 15 mJ; d = 3.95 mm; x = 0.15 mm). The residual stresses of EN-GJL 250 after RSP and SRSP are lower than those obtained for the EN-AW 7075 aluminum alloy [21]. The results of residual stress show the same trend as that observed for microhardness.

CONCLUSIONS

This study investigated the properties of preground EN-GJL 250 gray cast iron samples subjected to regular shot peening (RSP) and semi-random shot peening (SRSP). Based on the obtained results, it can be concluded that:

- the method of dimple creation affects the geometric structure, residual stress and microhardness of the surface;
- RSP yields lower values of surface roughness parameters than SRSP,
- the lowest values of surface roughness parameters were obtained after RSP conducted with the following technological parameters: E = 100 mJ, x = 0.3 mm, d = 14.3 mm,
- the Abbott-Firestone curve parameters *Rpk* and *Rk* are lower after RSP than after SRSP; an opposite trend can be observed for the *Rvk* parameter, parameters *Rpk* and *Rk* are after RSP from 5% to 64% lower than after SRSP;
- the microhardness and residual stresses on the surface of the EN-GJL 250 gray cast iron samples are higher after SRSP than after RSP (for microhardness the maximus difference is 7% and from residual stress the difference is from 2% to 16%).

The results have confirmed that the selection of the surface layer properties of gray cast iron EN-GJL 250 after regular shot peening and semi-random shot peening was well-chosen. However, for a wider application of these results, future works should investigate the RSP- and SRSP-induced residual stress of EN-GJL 250 together with the abrasive wear resistance of this material.

REFERENCES

1. Zhang P., Lindeman J. Influence of shot peening on high cycle fatigue properties of the high – strength magnesium alloy AZ80. Scripta Materialia 2005; 52(6): 485–490.
2. Skoczylas A., Zaleski K. Study on the surface layer properties and fatigue life of a workpiece machined by centrifugal shot peening and burnishing. Materials 2022; 15: 6677.
3. Avcu Y. Y., Iakovakis E., Guney M., Çalım E., Özkılınç A., Abakay E., Sönmez F., Koç F.G., Yamanoğlu R., Cengiz A., Avcu E. Surface and tribological properties of powder metallurgical Cp-Ti titanium alloy modified by shot peening. Coatings 2023; 13(1): 89.
4. Walczak M., Szala M., Okuniewski W. Assessment of corrosion resistance and hardness of shot peened X5CrNi18-10 steel. Materials 2022; 15(24): 9000.
5. Barahate V., Govande A.R., Tivari G., Sunil B.R., Dumpala R. Parameter optimization during single roller burnishing of AA 6061-T6 alloy by design of experiments. 2022; 50: 1967–1970.
6. Korzynski M., Dudek K., Korzynska K. Effect of slide diamond burnishing on the surface layer of valve stems and the durability of the stem-graphite seal friction pair. Applied Sciences 2023; 13: 6392.
7. Ferencsik V., Varga G. The influence of diamond burnishing process parameters on surface roughness of low-alloyed aluminiumworkpieces. Machines 2022; 10: 564.
8. Wang C., Tao X., Sun K., Wang S., Li K., Deng H. On the sensitivity of the three dimensional random representative fnite element model of multiple shot impacts to the SP induced stress feld, Almen intensity, and surface roughness. The International Journal of Advanced Manufacturing Technology 2023; 125: 2549–2567.
9. Kowalik M., Trzepieciński T., Kukiełka L., Paszta P., Maciąg P., Legutko S. Experimental and numerical analysis of the depth of the strengthened layer on shafts resulting from roller burnishing with roller braking moment. Materials 2021; 14(19): 5844.
10. Grochała D., Berczyński S., Grzadziel Z. Modelling of burnishing thermally toughened X42CrMo4 steel with a ceramic ZrO2 ball. Archives of Civil and Mechanical Engineering 2017; 17(4): 1011–1018.
11. Kalisz J., Żak K., Wojciechowski S., Gupta M.K., Krolczyk G.M. Technological and tribological aspects of milling-burnishing process of complex surfaces. Tribology International 2021; 155: 106770.
12. Qian W., Huang S., Yin X., Xie L. Simulation analysis with randomly distributed multiple projectiles and experimental study of shot peening. Coatings 2022; 12(11): 1783.
13. Skoczylas A., Zaleski K., Zaleski R., Gorgol M. Analysis of surface properties of nickel alloy elements exposed to impulse shot peening with the use of positron annihilation. Materials 2021; 14(23): 7328.
14. Skoczylas A., Zaleski K. Effect of centrifugal shot peening on the surface properties of Laser-Cut C45 Steel Parts. Materials 2019; 12(21): 3635.
15. Maleki E., Unal O., Kashyzadehc K.R., Bagherifarda S., Guaglianoa M. A systematic study on the effects of shot peening on a mild carbon steel: Microstructure, mechanical properties, and axial fatigue strength of smooth and notched specimens. Applied Surface Science Advances 2021; 4: 100071.
16. Skoczylas A. Vibratory shot peening of elements cut with abrasive water jet. Advances in Science and Technology Research Journal 2022; 16(2): 39–49.

17. Das T., Erdogan A., Kursuncu B., Maleki E., Unal O. Effect of severe vibratory peening on microstructural and tribological properties of hot rolled AISI 1020 mild steel. Surface and Coatings Technology 2020; 403: 126383.
18. Kulisz M., Zagórski I., Matuszak J., Kłonica M. Properties of the surface layer after trochoidal milling and brushing: Experimental and artificial neural network simulation. Applied Sciences 2020; 10: 75.
19. Matuszak J., Zaleski K., Ciecieląg K., Skoczylas A. Analysis of the effectiveness of removing surface defects by brushing. Materials 2022; 15: 7833.
20. Zaleski K. The effect of shot peening on the fatigue life of parts made of titanium alloy Ti-6Al-4V. Eksploatacja i Niezawodność – Maintenance and Reliability 2009; 4: 65–71.
21. Matuszak J., Zaleski K., Skoczylas A., Ciecieląg K., Kęcik K.: Influence of semi – random and regular shot peening on selected surface layer properties of aluminum alloy. Materials 2021; 14(24): 7620.
22. Wu J., Wei P., Liu H., Zhang B., Tao G. Effect of shot peening intensity on surface integrity of 18CrNiMo7-6 steel. Surface and Coatings Technology 2021; 421: 127194.
23. Takahashi K., Osedo H., Suzuki T., Fukuda S. Fatigue strength improvement of an aluminum alloy with a crack-like surface defect using shot peening and cavitation peening. Engineering Fracture Mechanics 2018; 193: 151–161.
24. Ongtrakulkij G., Khantachawana A., Kajornchaiyakul J., Kondoh K. Effects of the secondary shot in the double shot peening process on the residual compressive stress distribution of Ti–6Al–4V. Heliyon 2022; 8(1): e08758.
25. Ji S., Roberts K., Fan Z. Effect of shot peening on fatigue performance of ductile iron castings. Materials Science and Technology 2002; 18: 193–197.
26. Ochi Y., Masaki K., Matsumura T., Sekino T. Effect of shot–peening treatment on high cycle fatigue property of ductile cast iron. International Journal of Fatigue 2001; 23: 441–448.
27. Uematsu Y., Kakiuchi T., Tokaji K., Nishigaki K., Ogasavara M. Effects of shot peening on fatigue behavior in high speed steel and cast iron with spheroidal vanadium carbides dispersed within martensitic-matrix microstructure. Materials Science and Engineering: A. 2013; 561: 386–393.
28. Bagherifard S., Fernandez-Pariente I., Ghelichi R., Guagliano M. Effect of severe shot peening on microstructure and fatigue strength of cast iron. International Journal of Fatigue 2014; 65: 64–70.
29. Zammit A., Mhaede M., Grech M., Abela S., Wagner L. Influence of shot peening on the fatigue life of Cu–Ni austempered ductile iron. Materials Science and Engineering: A. 2012; 545: 78–85.
30. Silva K.H.S., Carneiro J.R., Coelho R.S., Pinto H., P. Brito P. Influence of shot peening on residual stresses and tribological behavior of cast and austempered ductile iron. Wear 2019; 440–441: 203099.
31. Zammit A., Abela S., Wagner L., Mhaede M., GrechM. Tribological behaviour of shot peened Cu–Ni austempered ductile iron. Wear 2013; 302(1–2): 829–836.
32. Zammit A., Abela S., Wagner L., Mhaede M., Wan R., Grech M. The effect of shot peening on the scuffing resistance of Cu-Ni austempered ductile iron. Surface and Coatings Technology 2016; 308: 213–219.
33. Zhan K., Zhang Y., Bao L., Yang Z., Zhao B., Vincent Ji V. Surface characteristic and wear resistance of QT-700-2 nodular cast iron after laser quenching combing with shot peening treatment. Surface and Coatings Technology 2021; 423: 127589.
34. Maleki E. Modeling of severe shot peening effects to obtain nanocrystalline surface on cast iron using artificial neural network. Materials Today: Proceedings 2016; 3(6): 2197–2206.
35. Feng A., Wei Y., Liu B., Chen C., Pan X., Xue J. Microstructure and mechanical properties of composite strengthened high-chromium cast iron by laser quenching and laser shock peening. Journal of Materials Research and Technology 2022; 20: 4342–4355.
36. González J., Peral L.B., Zafra A., Fernández-Pariente I. Influence of shot peening treatment in erosion wear behavior of high chromium white cast iron. Metals 2019; 9(9): 933.